Robust control of a flexible arm

Report of apprenticeship:

Robust control of a Flexible Arm.

By: M.J. v/d Molengraft

DCT 2001-34

9 July 2001

Supervised by:
Prof. Dr. Ir. S. Carabelli
Prof. Dr. Ir. M. Steinbuch

1 Introduction

In factories nowadays robots are commonly used. They are able to lift heavy weights, move fast with high precision and are able to work in environments where human beings are not. In space it is this last advantage that makes the use of robots interesting. Robots however are rather heavy and in space applications one of the most important factors is the weight. The price to bring an extra kilogram up in space is very high. This is why we want the robot to be as light as possible. A major disadvantage of reducing the weight is that resonances occur at lower frequencies, i.e. making the control design more difficult.

One idea is to use piezo elements to achieve good performance in the presence of these frequencies. These piezo elements will be placed on the robot arm to measure the deformation due to the flexibility and to counteract this deformation.

The controllers presented in this report do not include the piezo elements yet. The main goal was to see what performance could be obtained using only one input (the torque) and one output (the angle). A lead lag filter and two H_∞ designs will be presented and compared with the use of a simulator and measurements on the real system. A second goal of this research was to see if the simulator describes the behavior of the real system correctly. If it does, information not available trough measurements can be obtained with the use of the simulator.

In the next chapter the system will be presented. In chapter 3 the controller designs and a short evaluation of these designs will be shown. The simulator results are shown in chapter 4 and the measurements on the real system in chapter 5. Finally some conclusions and recommendations are given in chapter 6.

2 System

The system consists of a flexible beam driven by a motor with a mass on the tip of the link. Due to the flexibility of the link there will be some deformation (Vd_{tip}) at the tip. The input to the system is the torque applied to the motor. The output is the angle (θ_{hub}). A schematic overview of the system is presented in figure 2.1.

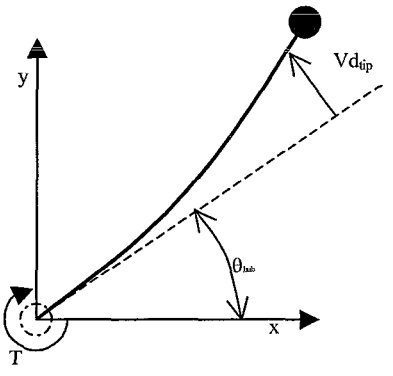

Figure 2.1: Schematic overview of the system

The flexible arm is, in essence, a double integrator perturbed by the resonances at the modal frequencies. In the real system there are infinitely many modal frequencies, in the model however it is impossible to take all these frequencies into account. Therefore the model can only be an approximation of the real system (as always). In this case however good information about the model error is available. The model is said to be good, thus the only model error is the fact that there are more resonance frequencies then that accounted for. Below is a bode plot for the 3rd and 5th order modal models. They are the same up to the 4th modal order. After that the difference is obvious.

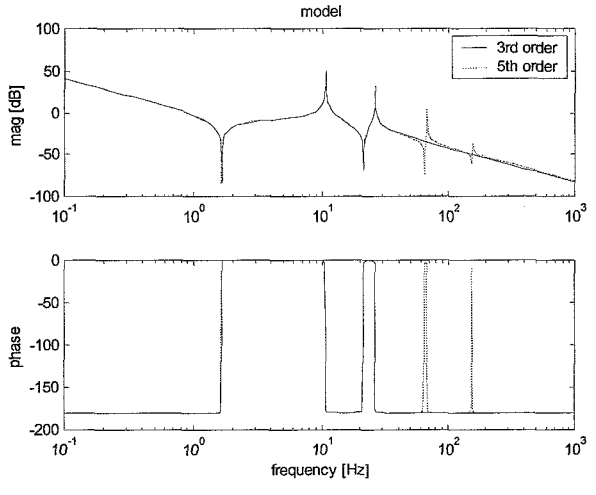

Figure 2.2: Bode plot model 3rd and 5th order

This means that checking the controller performance with a higher order model than used for the design of this controller would give a good impression of the performance with the real system. For the design of the different controllers a 3rd order modal model will be used. Meaning a 6th order model, since every modal

frequency results in to two poles. For the plant model a 5th order modal model is used. The models are in state space notation.

$$\dot{x} = A_p x(t) + B_p u(t) + v(t)$$
$$y = C_p x(t) + D_p u(t) + w(t) \qquad (!.1)$$

For the used models there is no direct feed through from input u to measurement y ($D_p = 0$). The vector $v(t)$ is the state disturbance and the vector $w(t)$ the measurement noise.

There are two different configurations to be considered. The first situation is one without a mass on the tip of the link. The second and more important one includes the mass on the tip. Resonance frequencies are different for the two situations and there is a significant change in the gain of the model at lower frequencies, as can be seen in the bode plot below.

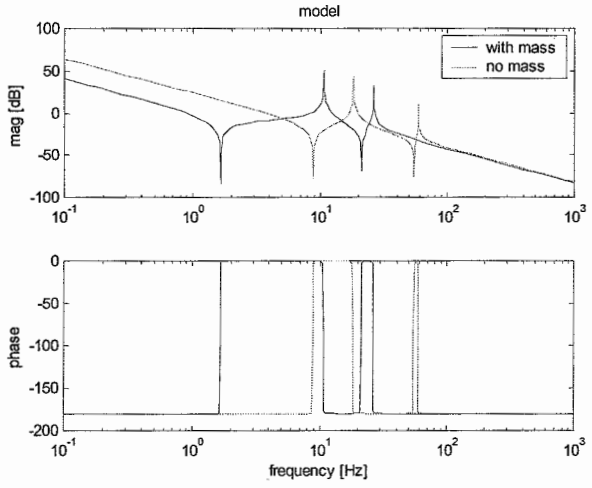

Figure 2.3: Bode plot system with and without mass

The situation with the mass on the tip is the more interesting one, since moving a flexible arm without anything attached to the tip seems rather pointless. The situation with the mass will put a higher demand on the controller and the actuator simply because of the inertia of the mass. The attainable bandwidth will be lower as well, since the first resonance peak occurs at a lower frequency. This report focuses on the situation with the mass but since the real system did not contain this mass yet, results are also shown for the no-mass configuration.

3 Controller design.

The poles and zeros of the modal models are close to the imaginary axis, so they are very lightly damped. As a result the system is close to instability. A way of counteracting the instability is output feedback. Just using simple unitary feedback does not do the trick, since unity feedback does not add damping to the system. For this a D-action is needed.

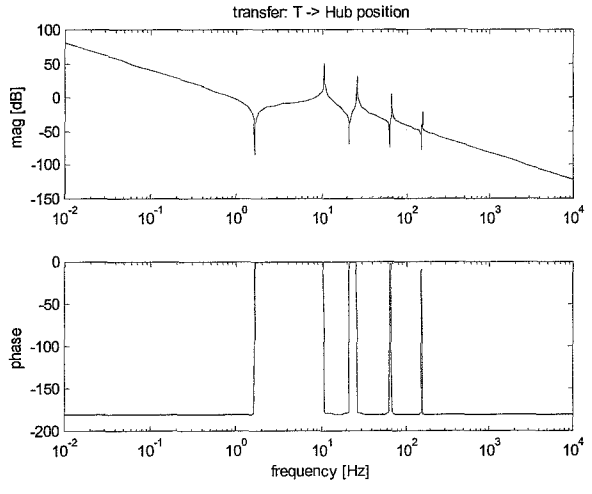

Figure 3.1: Bode plot system

In order to get a grip on the characteristics of the system and to see what level of performance a 'simple' controller can achieve, a lead lag filter is designed on the error of the system using only one input and one output. After this 'simple' controller is designed an H_∞ approach is used to achieve a possibly better controller. Efforts have been made on a linear quadratic gausian regulator (LQG) approach. Since there is not enough information to properly design the different weightings in this approach and results were not that promising this approach will not be discussed in this report.

3.1 Lead lag filter.

Since the main objective of the control law should be to add damping to the resonance frequencies, the first controller is designed to be a lead lag filter with a first order low pass filter for frequencies higher than 1 kHz. The lead lag is designed around 10 Hz, resulting in a filter having a zero at 1 Hz and a pole at 60 Hz. The bode plots of the filter and the closed loop system of the 5th order modal model in combination with the filter are shown in figure 3.2. Beware of the difference in the frequency range between de bode plot of the controller and the closed loop system in comparison to the bode plots in chapter 2. Whereas the frequency range for the controller and the closed loop is set to catch the characteristics of the different controllers, the range in chapter 2 was set around the resonance peaks.

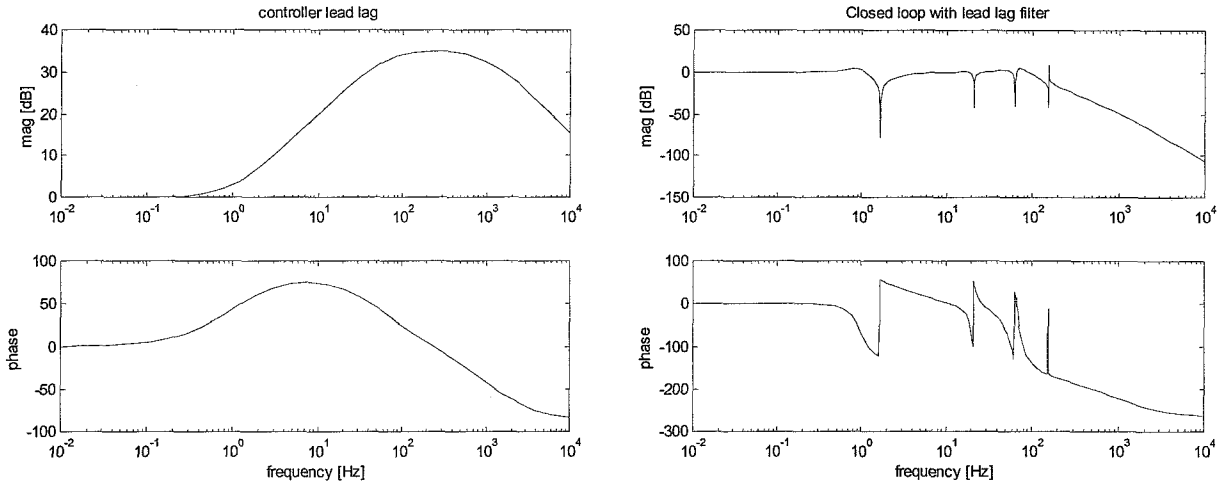

Figure 3.2: Bode plot lead lag filter and closed loop

The positive resonance peaks (resulting from a pole-pair) are almost gone, while the negative peaks (resulting from a zero-pair) remain almost unchanged. A consequence of these negative peaks in the complementary sensitivity is the phase lag associated with the peak. These phase lags will have a big influence on tracking performance. Both the controller and the closed loop are stable. Results for the system without a mass on the tip are presented in appendix A.

3.2 H_∞ control

In the former section a lead lag filter was used to add damping to the system. The main aim was to add damping to the resonance peaks. In this section two H_∞ designs will be discussed. The first design is a rather standard one, with weightings on the error and the actuator command. The second one contains an extra weighting on the tip deflection in order to minimize this deflection.

3.2.1 Standard design.

With the use of the function Hinfdes.m in the diet toolbox in MatLab a control law can be obtained [1]. The function is a fast working simple approach only suitable for siso systems. Appealing about the function is the fact that the 'standard plant' and the filters needed for H_∞ design, are defaults and do not have to be designed by the user. The syntax of the function is as follows.

$[A_c, B_c, C_c, D_c]$ = hinfdes (A_p, B_p, C_p, D_p, hz, hzbb, hzf, kS, kT,mr)

with: A_c, B_c, C_c, D_c = state space matrices controller
A_p, B_p, C_p, D_p = state space matrices plant
hz = frequency vector for plotting [Hz]
hzbb = desired bandwidth [Hz]
hzf = integral and low-pass frequencies, default: 16
kS = performance weighting, default: 1
kT = robustness weighting, default: 1
mr = controller reduction, default: 0.1

After trying a set of weightings, evaluating the resulting controller and adjusting the weightings a couple of times, the following values were used for the design of the controller for the system with a mass on the tip of the link:

hzbb = 9
hzf = 16
kS = 0.01

kT = -1

A negative value for kT forces the function to use a 1st order instead of a 2nd order low-pass filter. A positive value for kS results in a single integral action, while a negative value would result in a double integral action. The achieved value $\gamma = 2.69$ and the controller, after some balanced reduction is of the 8th order (without reduction the order would be 6+2+2 = 10). The bode plot of the controller and the closed loop system are as pictured below (with the same frequency ranges as used in the previous section).

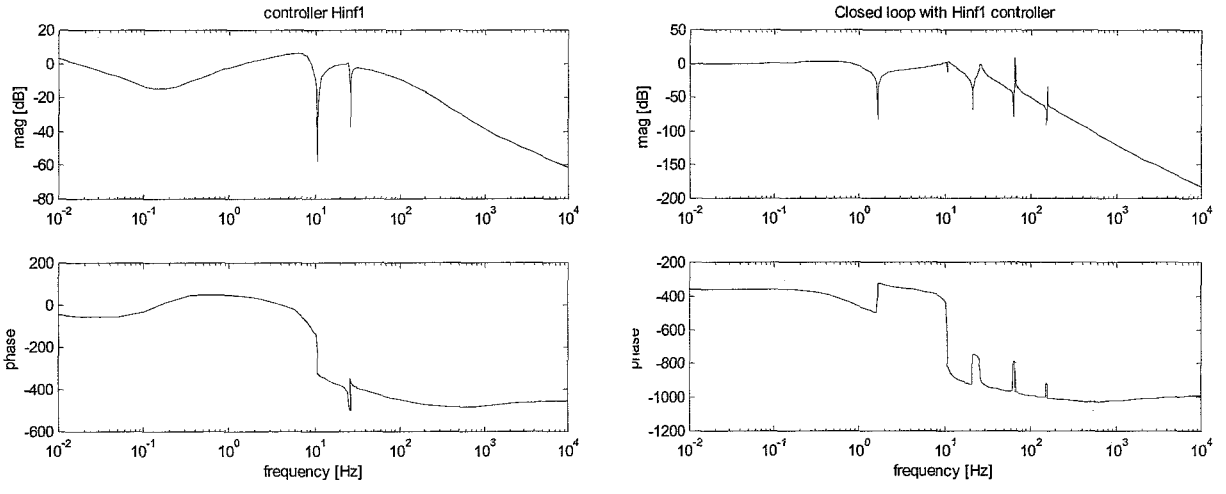

Figure 3.3: Bode plot H_∞ controller and closed loop

De function makes use of a standard plant consisting of two inputs and two outputs [2]. Only the outputs are weighted. The configuration of the standard plant is shown below.

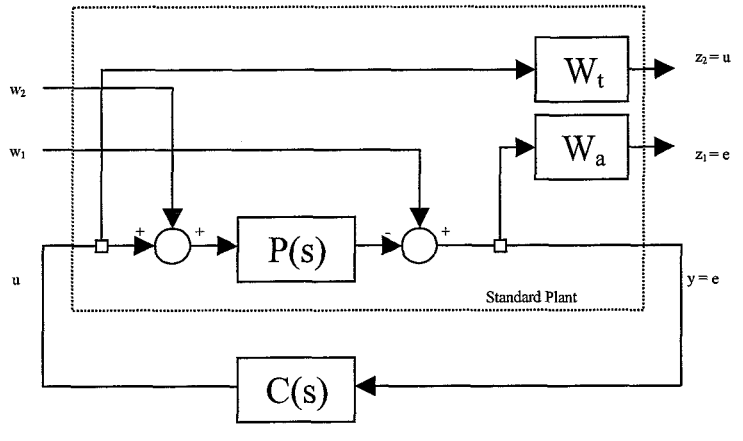

Figure 3.4: Standard plant

The standard plant can be formulated as z=G*w, with z being the output(s), G the standard plant and w the input(s). With this notation the standard plant can be formulated as below.

$$z = \begin{bmatrix} \tilde{e} \\ \tilde{u} \\ y \end{bmatrix} = \begin{bmatrix} W_a & -W_a P & -W_a P \\ 0 & 0 & W_t \\ I & -P & -P \end{bmatrix} \cdot \begin{bmatrix} w_1 \\ w_2 \\ u \end{bmatrix} = G \cdot w \qquad (3.1)$$

The H_∞ design problem can be formulated as follows.

$$\min_{Cstab} \sup_{w \in L_2} \frac{\|z\|_2}{\|w\|_2} = \min_{Cstab} \|M(C)\|_\infty \qquad (3.2)$$

$$with \ldots M(C) = \begin{bmatrix} W_a S & -W_a SP \\ W_t CS & -W_t CSP \end{bmatrix}$$

The standard plant thus has weightings on the sensitivity (S and PS), the control sensitivity (R=CS) and the complementary sensitivity (T=CSP). This in contrast to a setup, only containing weightings on S and R (or T). A big advantage of this setup is the lower complexity of the problem. For the controller to have integral action, meaning a slope of +3 in the sensitivity (for a double integrator system), in the general setup a 3rd order weighting (acting on S) is needed. In the setup used here a 1st order weighting (on SP) is sufficient to achieve the wanted integral action.

The used settings result in the following weightings on the performance and the robustness.

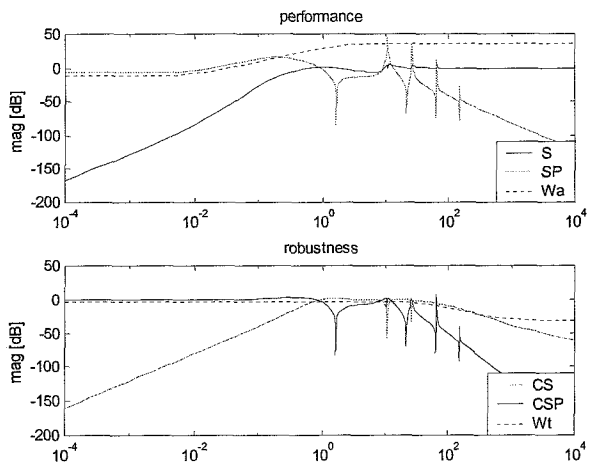

Figure 3.5: Weightings

The weighting on the performance looks like it could be improved. Efforts to do so however did not improve the total performance significantly. The designed controller for the situation without a mass on the tip along with the results is presented in appendix A. The design parameters are the same with the exception of the bandwidth. As the bandwidth for the situation with mass is set at 9 Hz, the bandwidth for the situation without the mass is set to 27 Hz. This is possible since the resonance peaks are at higher frequencies and the system has a higher gain at low frequencies.

3.2.2 Extra weighting on Tip deflection

In the previous two sections controllers were presented, designed on the error between the reference and θ_{hub}. Since the real interest lies at the position of the tip rather than on that of the rotor, it is sensible to take account for this tip position. However, since only measurements of the rotor position are available, it is not possible to design a controller that makes a direct use of this position. With H_∞, on the other hand, indirect use of the position is.

The available finite element model not only contains information about the rotor position (and the piezo voltages), but on the tip position and deflection as well. The tip position is the signal to be controlled. Incorporation of the position however would ask for a setup with a tip reference next to the rotor reference. This poses no big problem, since there is a logical relationship between these two references. The model, however already contains the tip position error, also called the tip deflection (caused by the flexibility of

the link). The control law should minimize this tip deflection using only the rotor position signal. Figure 3.6 shows the transfer from the torque (T) to the tip deflection (V_d).

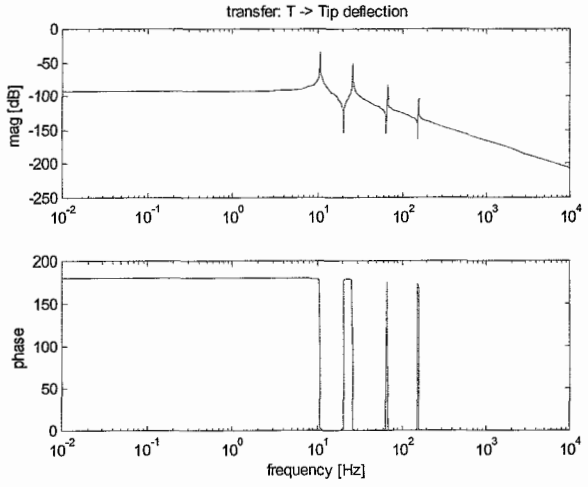

Figure 3.6: Bode plot transfer T -> Tip deflection

A way to achieve a controller with above specification is to put an extra weighting on this deflection and to loosen the other weightings if necessary. The standard plant for this design is pictured below.

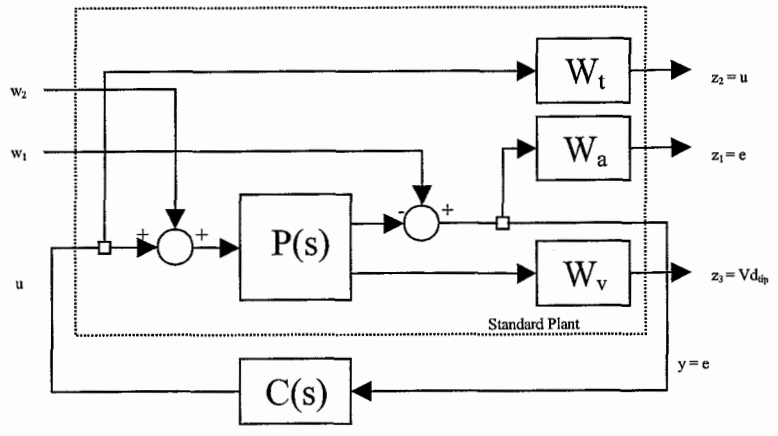

Figure 3.7: Standard plant with weighting on tip deflection

Using the same notation as in the previous section, the standard plant is:

$$z = \begin{bmatrix} \tilde{e} \\ \tilde{u} \\ \tilde{V}_d \\ y \end{bmatrix} = \begin{bmatrix} W_a & -W_a P_1 & -W_a P_1 \\ 0 & 0 & W_t \\ 0 & W_v P_2 & W_v P_2 \\ I & -P_1 & -P_1 \end{bmatrix} \cdot \begin{bmatrix} w_1 \\ w_2 \\ u \end{bmatrix} = G \cdot w \tag{3.3}$$

The H_∞ design problem for this standard plant is as follows.

$$\min_{Cstab} \sup_{w \in L_2} \frac{\|z\|_2}{\|w\|_2} = \min_{Cstab} \|M(C)\|_\infty \tag{3.4}$$

$$with \ldots M(C) = \begin{bmatrix} W_a S & -W_a S P_1 \\ W_t C S & -W_t C S P_1 \\ W_v C S P_2 & W_v S P_2 \end{bmatrix}$$

The sensitivity S is the same as in the previous section, in the sense that it is the sensitivity from the reference signal to the tracking error (e = r-y). The plant is divided into two sub plants. P_1 is the transfer from the input u to the hub position $y = \theta_{hub}$, P_2 is the one from u to the tip deflection (Vd_{tip}).

The upper four elements of M(C) are the same for both standard plants. The difference is in the lower part of M(C), where the extra weighting on the tip deflection is added. The first term $M(3,1) = CSP_2$ is similar to the term $M(2,2) = CSP_1$, while $M(3,2) = SP_2$ is similar to $M(1,2) = SP_1$. Meaning that the weighting on the tip deflection results in a performance and a robustness weighting for this deflection. The main wish is to improve performance and for that reason the weighting W_v is designed to be similar to the weighting W_a. The weights on the performance and the robustness are loosened a bit compared to the previous design. Figure 2.7 shows the used weightings and the resulting plots for the elements of M(C).

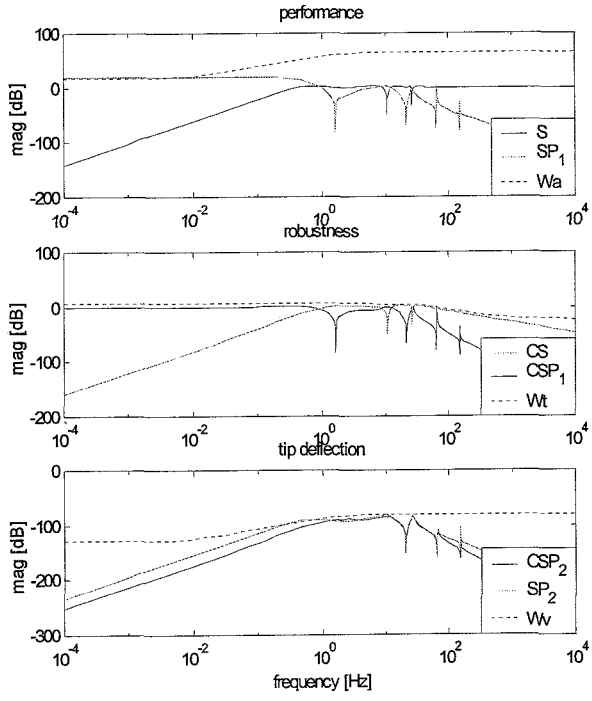

Figure 3.8: Weightings

The weighting used for the tip deflection has the same characteristics as the weight on the performance, the only difference being the gain. The controller and the closed loop response resulting from this setup are shown below.

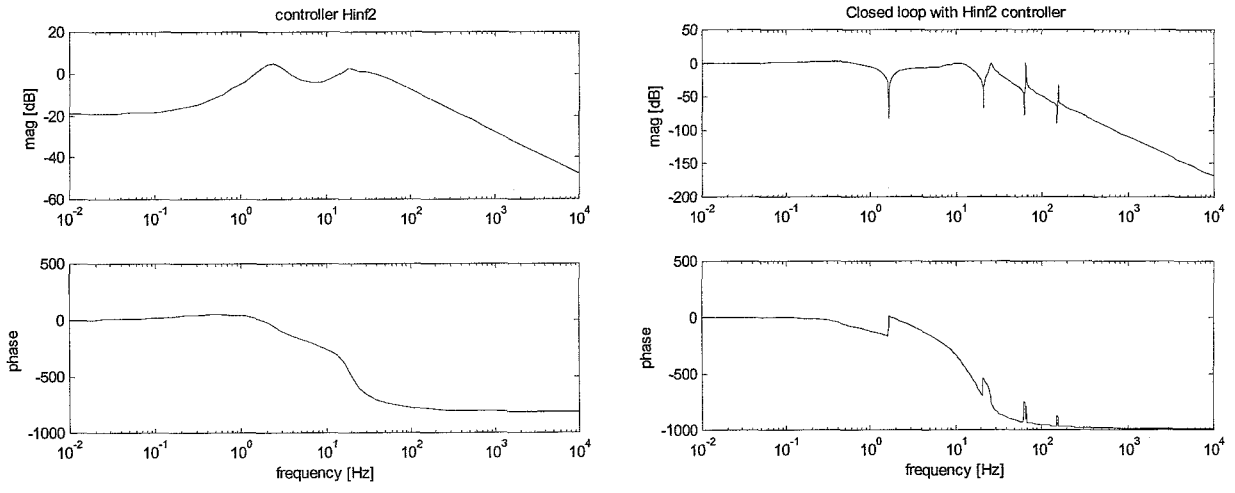

Figure 3.9: Bode plot H $_{\tilde{z}}$ controller and closed loop

The order of the resulting controller after reduction is 6 (without reduction it would have been 6+2+2+2=12). The controller seems to be a milder controller compared to the previous design. This is logical considering that for a lower tip deflection a lower actuator and thus control activity is required.

3.3 Evaluation controllers

In this section the controllers designed in the previous sections will be shortly evaluated. In order to do this, the sensitivities and the step responses for the three closed loop systems are shown and compared.

The sensitivities for the closed loop system with the different controllers are shown in figure 3.10.

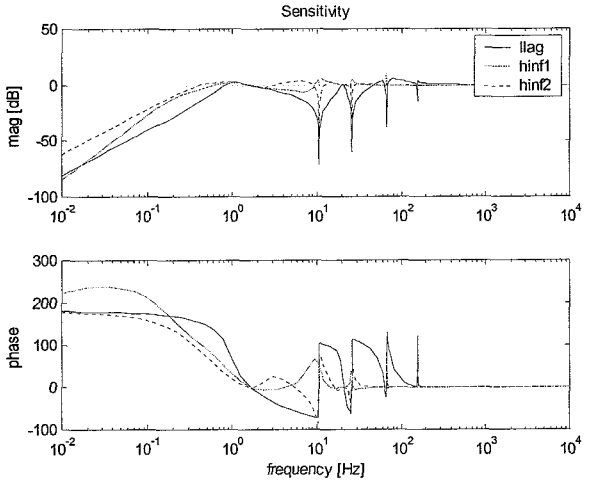

Figure 3.10: Sensitivities

For low frequencies the lead lag filter and the first H_∞ design have a lower gain than the second H_∞ design. These controllers have a higher gain than the second H_∞ design at higher frequencies. The cause of this lies in the Bode's sensitivity integral (also known as the Water Bed Effect) which states that the area under the 0 dB line equals the area above this line. With the first H_∞ design the modal frequencies are not

compensated as good as with the other designs. This can be seen in the step responses for the various closed loop systems.

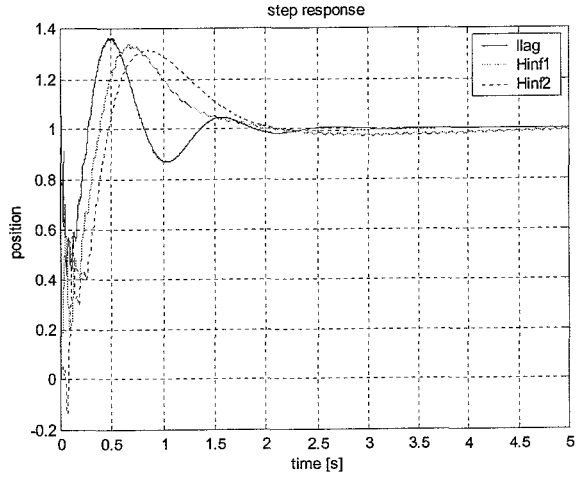

Figure 3.11: Step response position

Looking at the step-response it can be seen that the lead lag filter has a shorter rise time than the H_∞ designs. The settling time (with the demand being: error < 0.1%) however is close to 3.5 sec for both the lead lag as the second H_∞ approach (3.4 and 3.7 seconds respectively). The first H_∞ approach has a longer settling time (19 sec). The improvement obtained using the H_∞ design instead of the lead lag can be seen in the step response for the tip deflection. Here it can be seen that the second H_∞ design shows less oscillation compared to the lead lag filter.

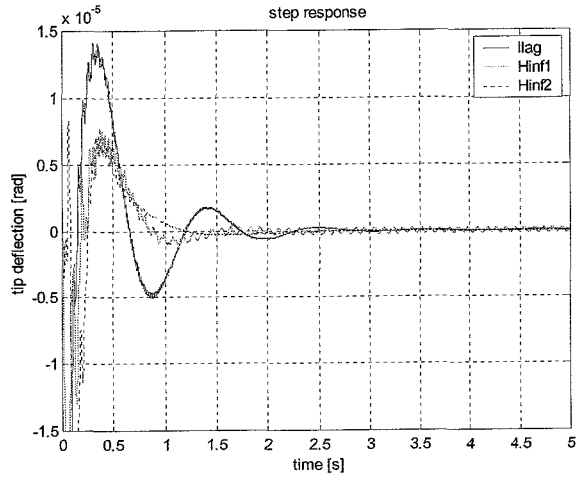

Figure 3.12: Step response tip deflection

The first H_∞ design shows an oscillation with a frequency around 10 Hz, corresponding to the first resonance peak or the second modal frequency. This resonance frequency is cancelled in the other designs. For the 3rd modal frequency at 20 Hz goes the same. Both H_∞ designs show an oscillation at the 4th modal frequency 67 Hz. The lead lag filter shows a lower gain at this frequency and a higher gain and therefore more oscillation at the 5th modal frequency 156 Hz. These last two modal frequencies were not accounted for in the controller design.

The step response for the Tip deflection shows that the H_∞ design with the weighting on the Tip deflection has the best results. It appears to have the lowest settling time. This is not entirely true, since there remains

an oscillation at the 4th modal frequency 67 Hz. The lead lag filter has as mentioned above a lower gain at this frequency. The H_∞ design shows a better result up to about 3.5 [s], after that the oscillations are smaller for the lead lag filter. This can be seen in figure 3.11 where the step responses for the tip deflection are shown from 3.5 to 4 [s]. The tip deflection at this point is very small for both designs, so the question rises what the influence of the difference will be.

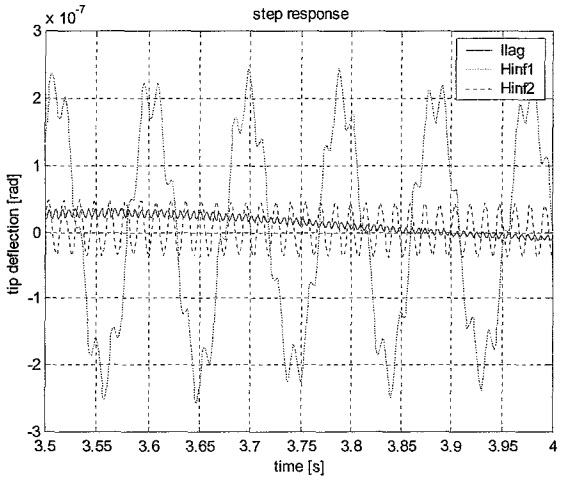

Figure 3.13: Step response tip deflection 3.5 - 4 [s]

4 Simulation

In this chapter simulation results for the controllers designed in the previous chapter will be shown. There are two major situations to be considered (apart from the mass- and no-mass situation), namely a situation where the simulation contains friction and the situation where the friction is not included. In the situation with friction, simulations are done with and without an integrator to cancel the friction. The simulation results for the no-mass situation are shown in appendix B.

4.1 Simulation without friction

The first simulation results are the results for the situation without friction. In figure 4.1 the results are shown for a simple reference signal containing an acceleration, a constant velocity and a deceleration over an angle of 75 degrees. The time range is set from 0 to 5 sec. This is done for better comparison with the results from the measurements (where only 5 sec could be measured) presented in the next chapter.

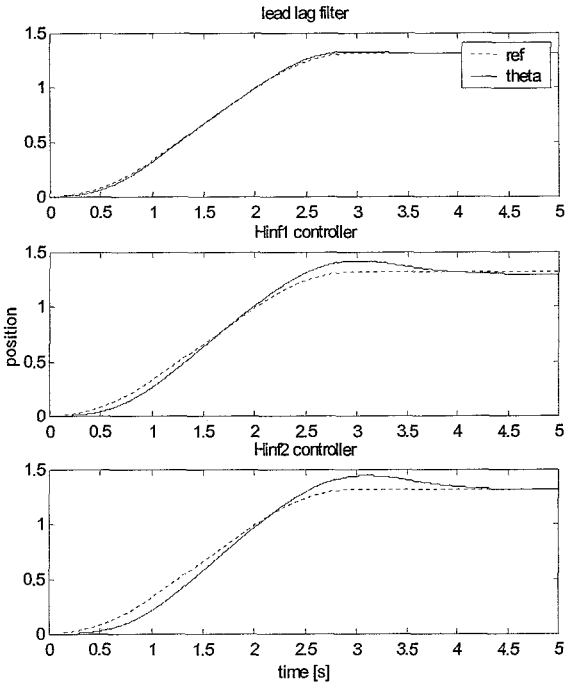

Figure 4.1: simulation of the position, without friction

The lead lag appears to have the smallest error and the smallest settling time. The lead lag reaches the end value of the reference signal (error < 0.1%) in 4.5 sec, where both H_∞ designs take 7.5 sec. The explanation for this lies in the fact that the lead lag has a higher gain compared to the H_∞ designs. The simulation results for the tip deflection are shown in figure 4.2.

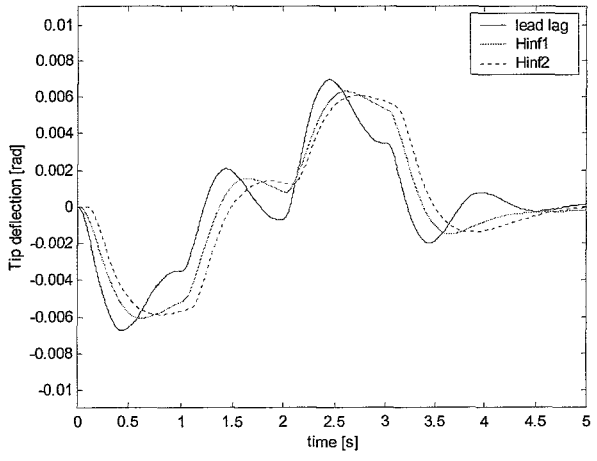

Figure 4.2: Simulation of the tip deflection, without friction

As was already shown in the last section of the previous chapter (with the use of the step responses), the tip deflection is smaller for the H_∞ designs compared to the lead lag filter. The lead lag filter and the second H_∞ design show the same settling time for the tip deflection, the first H_∞ design has a larger settling time. The H_∞ designs show a smoother graph than the lead lag filter, meaning less oscillation, which could be desirable. The cost is the higher settling time for the position.

4.2 Simulation with friction

The real system shows a lot of friction not compensated for by the controllers. At this point this friction is implemented in the simulator with a simple model containing coulomb and viscous friction.

$$y = \mathrm{sgn}(\dot{x}) \cdot \begin{cases} 36 \cdot |\dot{x}| & for\ |\dot{x}| < 0.05 \\ 0.02 \cdot |\dot{x}| + 1.8 & for\ |\dot{x}| \geq 0.05 \end{cases} \tag{4.1}$$

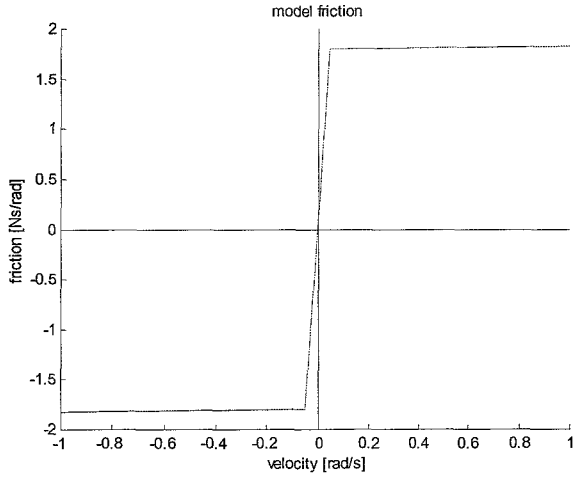

Figure 4.3: Model friction

This friction, especially the coulomb friction, is very high and will probably be too high for this application. The simulations for the situation without the friction resulted in a maximum value for the

torque around 1 Nm. With the friction incorporated the maximum is 3.3 Nm, which is more than 3 times as high.

The simulation results for this situation are shown in figure 4.3 and 4.4. The lead lag filter still shows good results. The H_∞ designs however degrade significantly. The settling time for the lead lag with friction is 5.5 sec and for the first H_∞ design it is 35 sec. The second H_∞ design takes about 39 seconds to reach the end value of the reference (again with the demand being: error < 0.1%). This compared to 4.5, 7.5 and 7.5 for the situation without friction. The reason for the lead lag to give the best results lies in the fact that this design has a higher gain. The difference in performance between the H_∞ designs can be explained by looking at the lower frequencies. The first H_∞ design shows a small integral action, resulting in a higher gain for these lower frequencies compared to the second H_∞ design.

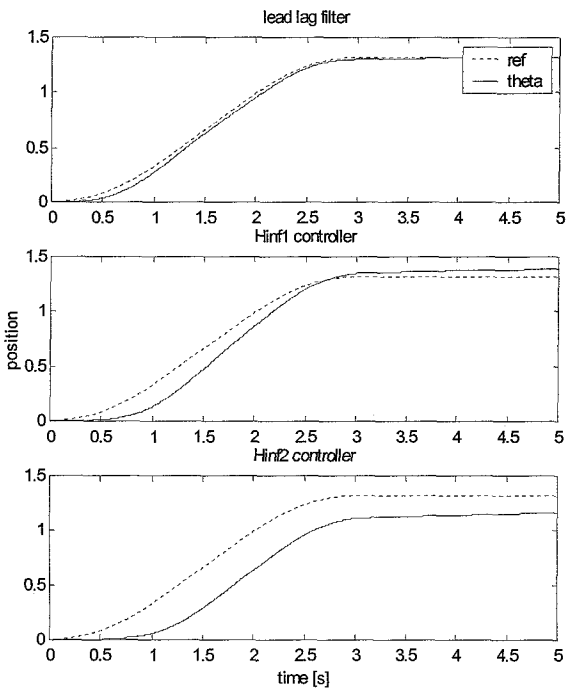

Figure 4.4: Simulation of the position, with friction

The simulation results for the tip deflection show that the friction causes oscillations with the first H_∞ design. These oscillations are at frequencies 10 and 67 Hz (the 2nd and the 4th modal frequency). The sensitivity plots in section 3.3 already showed that this design did not compensate these frequencies as good as the other designs.

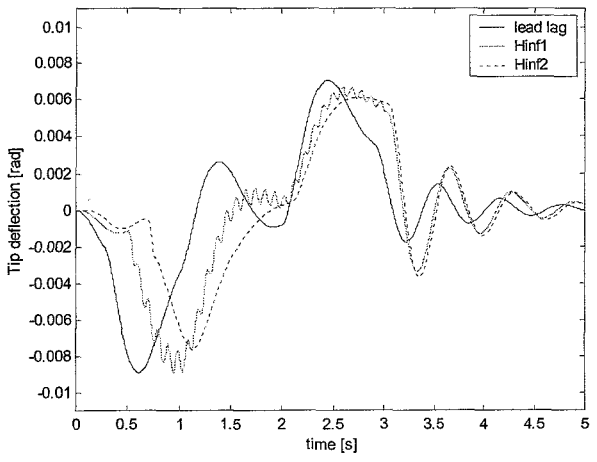

Figure 4.5: Simulation of the tip deflection, with friction

Another effect of the friction is the oscillation that occurs after the deceleration of the reference. Up to 3 seconds the behavior of the H_∞ designs is better then that of the lead lag filter. In fact there is not much difference with the no-friction case, apart from some oscillation with the first H_∞ design. After this the lead lag filter proves to be better, showing less oscillation. This can be accounted to the higher controller gain for the lead lag in comparison to the H_∞ designs.

The lead lag design appears to be the best controller for this situation. Although the tip deflection is smaller for the H_∞ designs in the first 3 seconds the lead lag shows better results from then on. Next to this the first H_∞ design shows more oscillation and both H_∞ designs have a significantly larger settling time.

4.3 Simulation with friction and integral action

To compensate for the friction and to guarantee zero steady state error, the three designs have been combined with an integral action, with its zero in 0.7 [rad/s] (or 0.11 [Hz]). The step response for the tip deflection remains almost unchanged. The one for the position is shown in figure 4.6. When compared to the step response without the integrator, it can be seen that this integral action causes for more overshoot and more oscillation, resulting in a larger settling time. For the situation without the integrator these settling times are 3.4, 19 and 3.7 seconds respectively, with the integrator this is 4.5, 19 and 8 seconds.

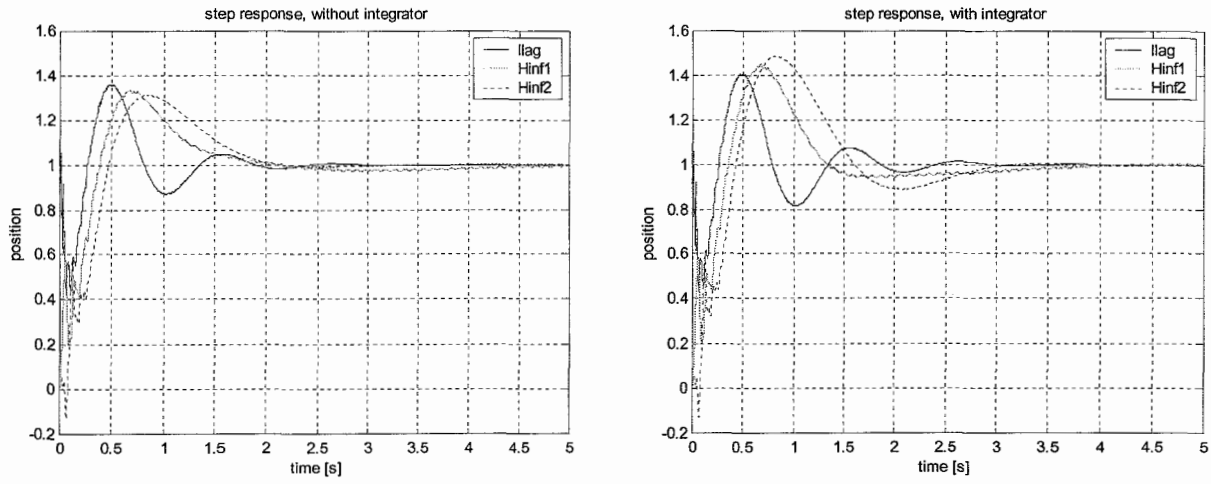

Figure 4.6: Step response position, with and withour integrator

The simulation results are shown in figures 4.7 and 4.8. Again the lead lag filter appears to have the best results. The settling time (error < 0.1%) for the lead lag filter with the integrator is 7 seconds, for the first H_∞ design it is larger than 50 seconds and for the second H_∞ design it is 41 seconds. The settling times for the H_∞ designs are very high compared to the lead lag filter, the explanation for this lies in the higher gain for the lead lag.

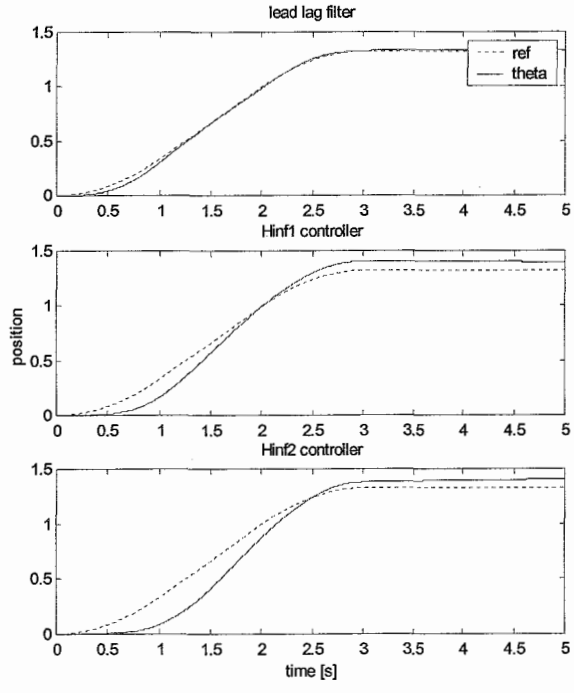

Figure 4.7: Simulation of the position, with friction and integrator

Looking at the simulation results for the tip deflection it can be seen that the advantages of the H_∞ designs are gone. In fact the lead lag shows the best results. The first H_∞ design shows even more oscillation compared to the situation without the integrator. Where the results for the situation without the integrator

were better for the H_∞ designs up to 3 seconds, here the lead lag filter shows the best result over the total time range. Thus the lead lag filter is the best option for this situation.

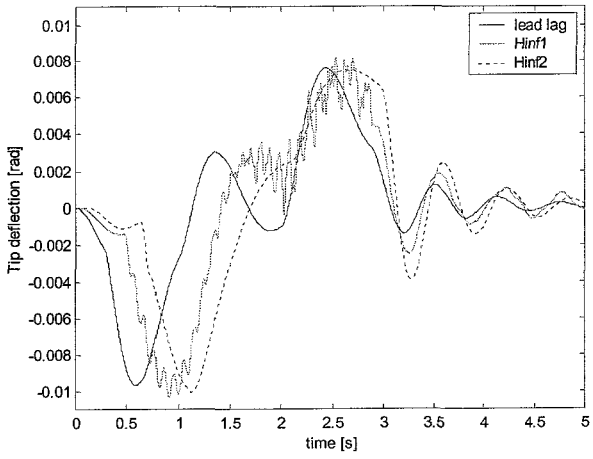

Figure 4.8: Simulation of the tip deflection, with friction and integrator

The lead lag filter appears to be the best controller for the situation with friction. The main reason for this is its higher gain. If the gain of the lead lag is lowered to resemble the gain of the H_∞ designs, the results for these H_∞ designs are better than those of the lead lag.

5 Measurements on the real system

In the previous chapter the designed controllers were tested trough simulations. The real system however can never be caught in simulations completely. The friction for instance is very hard to model. In this case a very simple model is used, which will clearly not describe the friction behavior correctly. Since the friction is very high compared to the torque needed for the movement of the arm, a small difference between the modeled and the real friction will have a big influence on the behavior.

The main goal of the measurements is to see how good the simulator approximates the real behavior. If there is not much difference between the measurements and the simulation, the simulator is reliable. If there is a lot of difference, the simulator does not describe the behavior correctly and will have to be altered to have any value. In the real system measurements of the tip deflection are not available. With the simulator this data can be generated, but if the simulator is not correct this data is useless. The simulation results for the situation without the mass on the tip are shown in appendix B.

The first H_∞ design turned out to be instable after implementation in the system. The reason for this lies in the order of the controller (8^{th} order). This appeared to be too high for the DSP system. Only the lead lag filter and the second H_∞ design were successfully implemented.

For the measurements 2 reference signals are used. The first is the same as used in the previous chapter. The second is a faster one (both over 75 degrees). In the following figures the measurements are shown together with the simulation results and the reference signal. Figures 5.1 and 5.2 show the results for the lead lag filter and the second H_∞ design without the integrator. The simulation results for the tip deflection are shown in figure B-4 for the first reference and B-7 for the second reference in appendix B. There appears to be a difference between the simulation results and the measurements. Incorrect modeling of the friction causes this difference. The friction is even higher than was accounted for in the model.

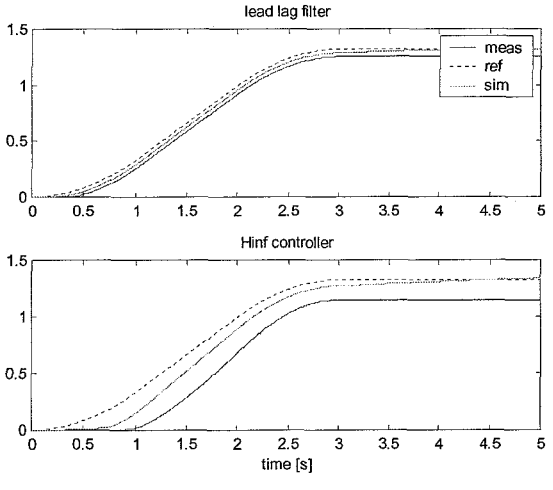

Figure 5.1: Reference 1, without integrator

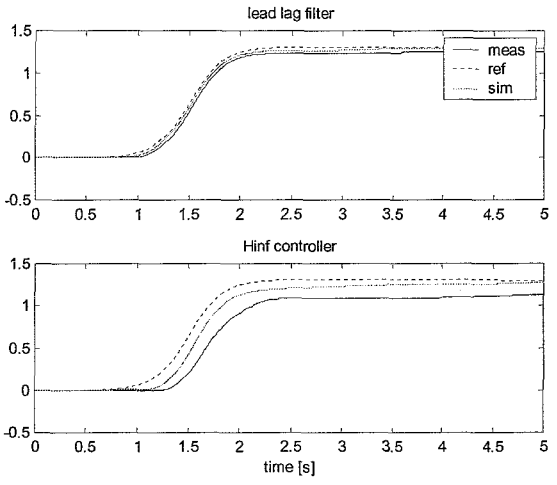

Figure 5.2: Reference 5, without integrator

Figures 5.3 and 5.4 show the results for the controllers combined with the integrator. The simulation results for the tip deflection are shown in figure B-6 and B-8 in appendix B. For the lead lag filter the measurements show much resemblance with the simulation results. With the H_∞ design however something is wrong. Since there is a pure integral action in the controller, the steady state error should be zero. This is not the case with the H_∞ design. The reason for this lies in the implementation. Where the first H_∞ design turned instable after implementation because of its high order (8^{th}) the second H_∞ design combined with the integrator appears to lose this integrator. The order of the second H_∞ design with the integrator is 7 and apparently too high for the DSP system.

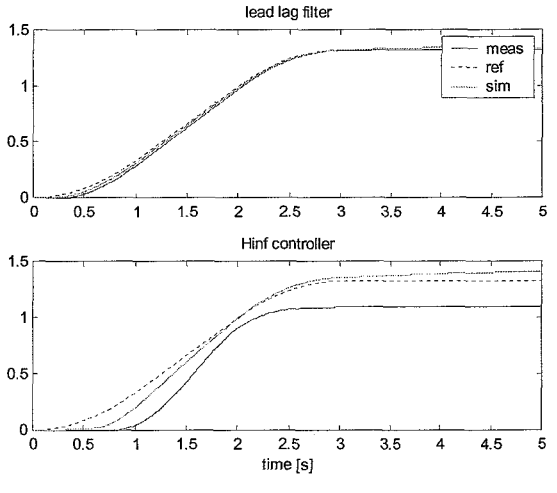

Figure 5.3: Reference 1, with integrator

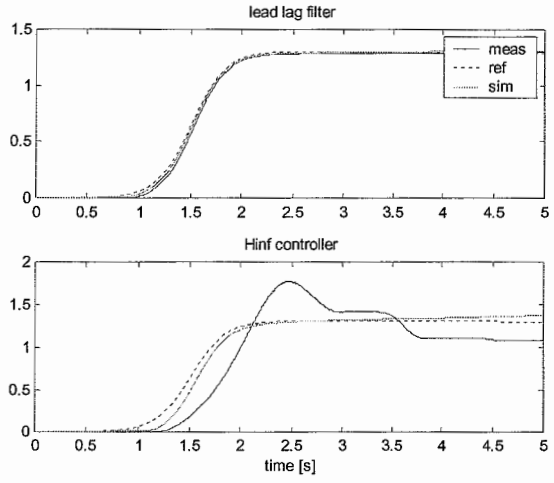

Figure 5.4: Reference 5, with integrator

From the measurements two conclusions can be drawn. The first is that the friction is not correctly modeled, the second is that the DSP system cannot handle controllers with an order higher than 6. With H_∞ the order of the controller (without order reduction) is that of the model plus the orders of the weighting filters used in the design. In this case a 3^{rd} order modal model meaning a 6^{th} order model is used for the design, thus it will be very hard to reach a controller with an order under 6. Using a lower order model for the system would give more freedom in designing the standard plant and the weights.

6 Conclusions and recommendations

The main goal of this report was to see what performance could be obtained using only one input and one output. A second goal was to see if the simulator describes the real system correctly.

The following conclusions can be drawn:

- The friction is too high for this application. With this high friction the 'simple' lead lag filter shows the best results. If the friction is low, the H_∞ designs are better.
- The extra weighting on the tip deflection results in a better design with less oscillation compared to the design without the extra weighting.
- The design of the weightings is a hard task and will be even harder if the piezo elements are to be used (more inputs and outputs means more weightings).
- The simulator does not describe the behavior of the real system correctly. The friction being the biggest problem.

Recommendations:

- A different motor should be used, showing less friction. This would improve the behavior of the system significantly.
- If the friction still plays an important roll, a better model for the friction should be obtained. This model can be used for the simulator as well as for the controller design, giving better information of the behavior of the system trough simulations and a better opportunity to design a good controller.
- For tracking a feed forward could be of use. This is not only useful for tracking however, but also for positioning. If the error remains small, the task of the controller is lighter and the controller output smaller.
- For high order controllers a different or an extra DSP system should be used. The current DSP system can only handle controllers up to order 6. For the MIMO case, where the piezo elements are used, H_∞ is a logical option. Using H_∞ however results in high order controllers.

Appendix A: Controllers for no-mass situation

- Lead lag filter:

The lead lag filter used for the no-mass situation is the same as used for the situation with the mass.

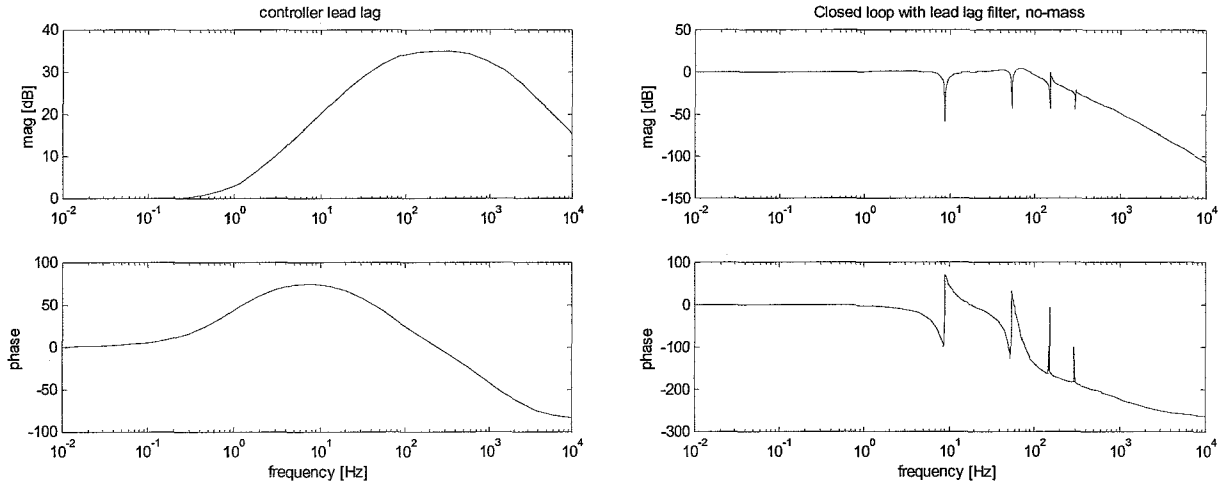

Figure A-1: Bode plot lead lag filter and closed loop

- First H_∞ design:

The parameters used for the first H_∞ design for the no-mass situation are the same as for the situation with the mass, except for the bandwidth. For the situation with the mass the bandwidth was set at 9 [Hz], for the no-mass situation it is 27 [Hz].

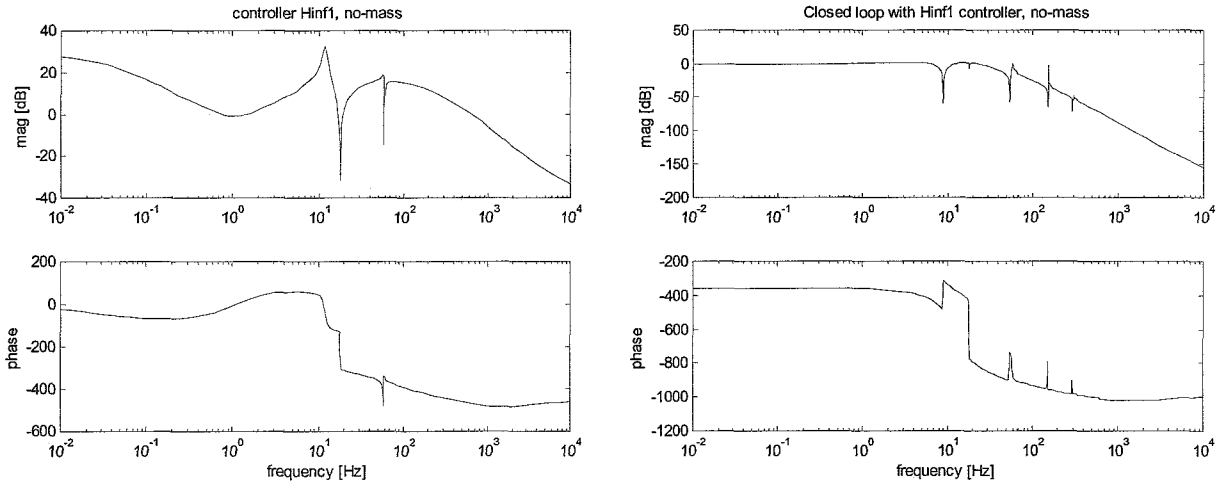

Figure A-2: Bode plot first H_∞ design and closed loop

- Second H_∞ design:

Here goes the same as for the first H_∞ design (bandwidth = 27 [Hz]).

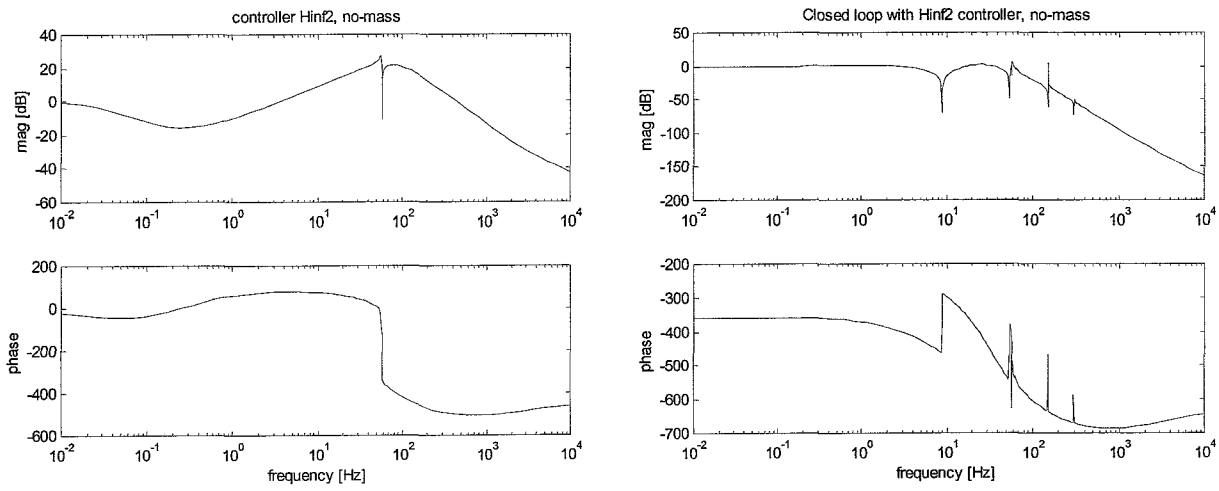

Figure A-3: Bode plot second H_∞ design and closed loop

- Sensitivities no-mass:

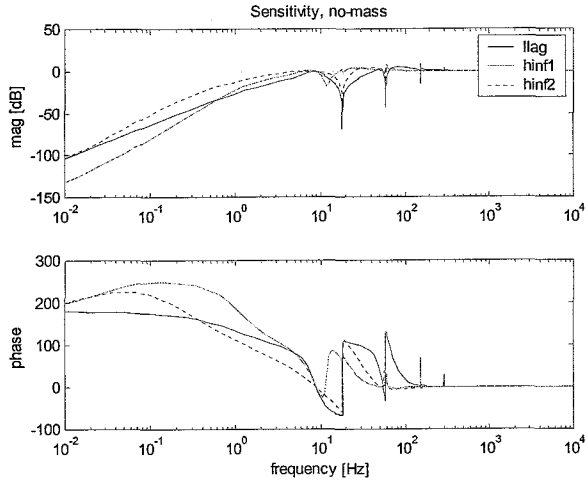

Figure A-4: Sensitivities no-mass situation

Appendix B: Simulation results for no-mass situation

- Simulation without friction:

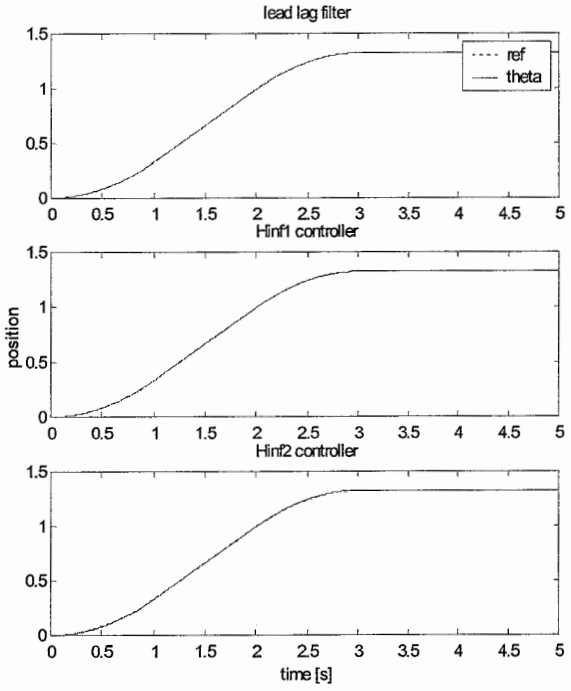

Figure B-1: Simulation of the position, without friction

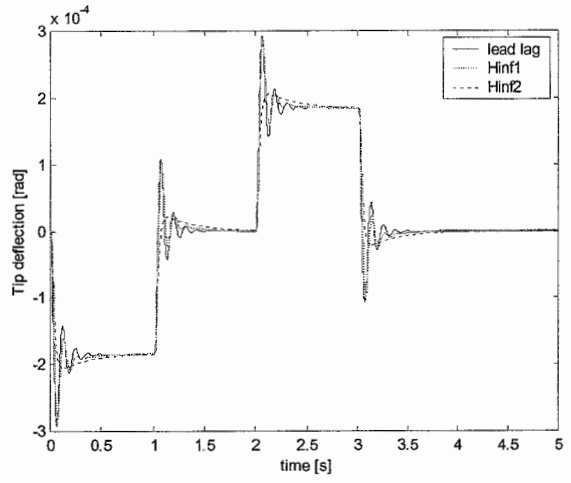

Figure B-2: Simulation of the tip deflection, without friction

As expected the second H_∞ design gives the best results for the situation without friction. The first H_∞ design does not differ much from the lead lag filter.

- Simulation with friction:

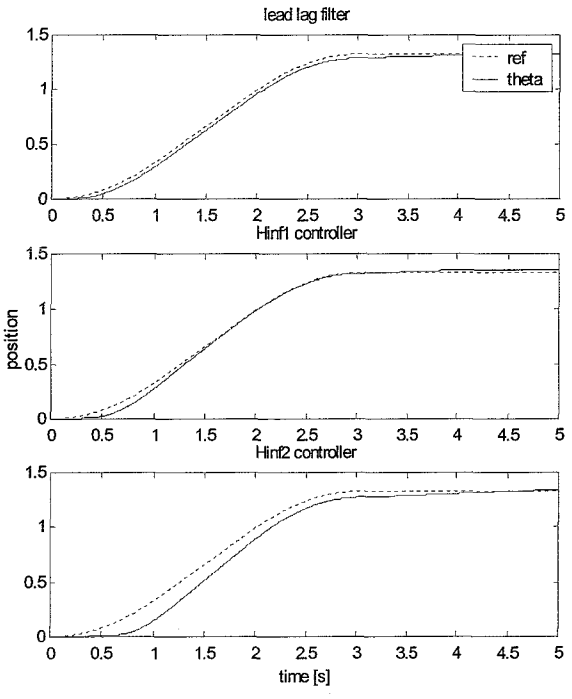

Figure B-3: Simulation of the position, with friction

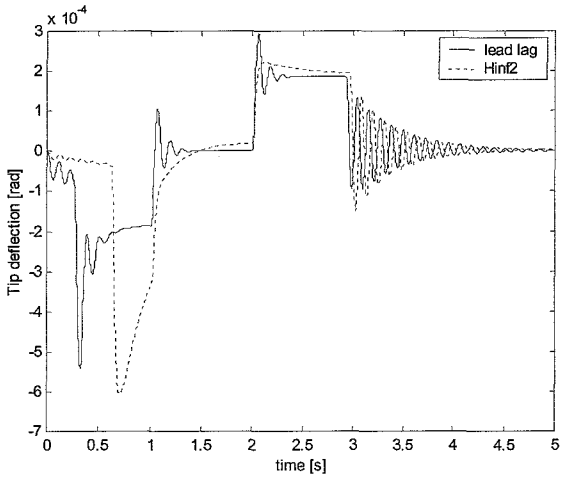

Figure B-4: Simulation of the tip deflection, with friction

The first H_∞ design resulted in a lot of oscillation in the tip deflection. For convenience only the results for the lead lag and the second H_∞ design are shown. The H_∞ design shows a better result for the tip deflection up to 3 seconds, after that the results for the lead lag and the H_∞ design are similar.

- Simulation with friction and integral action:

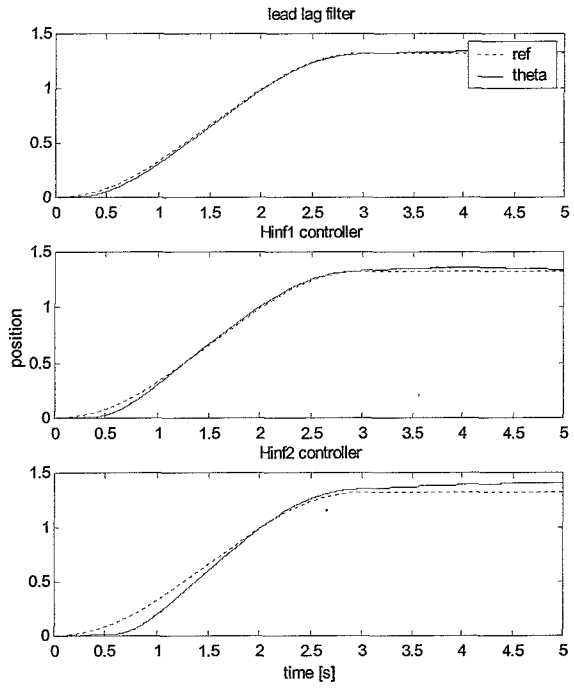

Figure B-5: Simulation of the position, with friction and integrator

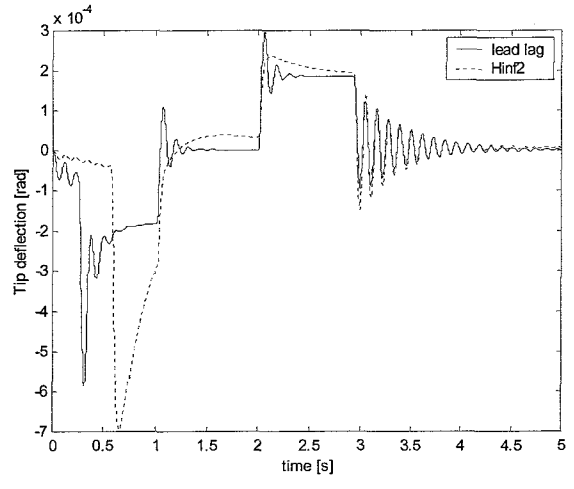

Figure B-6: Simulation of the tip deflection, with friction and integrator

Again the first H_∞ design shows much oscillation and is not shown for convenience. As in the previous case, the second H_∞ design shows a better result for the tip deflection up to 3 seconds.

- Simulation results for the tip deflection with reference 5

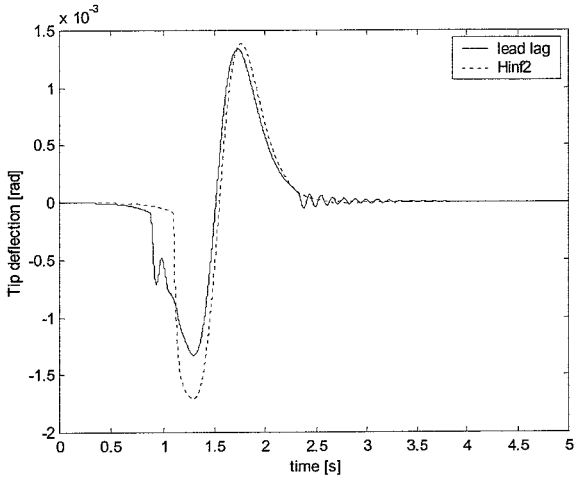

Figure B-7: Simulation of the tip deflection for the second reference, with friction

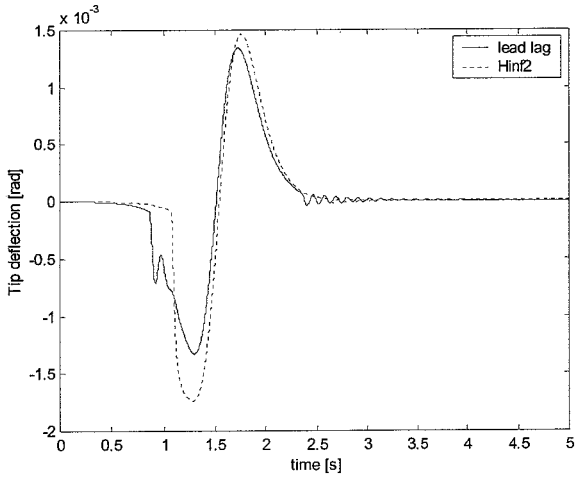

Figure B-8: Simulation of the tip deflection for the second reference, with friction and integrator

There is not much difference in the tip deflections for the two cases. It appears that the integrator does not influence the transfer from the input u to the tip deflection for the frequency range of the reference signal.

Bibliography

[1] M. Steinbuch, "Hinfdes.m", MatLab scriptfile, Eindhoven University of Technology, Dept. of Mechanical Engineering, Control Systems Technology Group

[2] P.J.M. Groos, "Robust control of a Compact Disc player", RWR-501-PG-93057-pg Technical note 143/93, Philips Electronics NV, 1993